THE NATURE OF SPACE WEATHERING IN SAMPLES FROM ASTEROID (162173) RYUGU REVEALED BY COORDINATED ANALYSIS. L.E. Melendez¹, M.S. Thompson¹, L.P Keller², S.A. Eckley³, M. Yesiltas⁴, and T.D. Glotch⁴, Department of Earth, Atmospheric, and Planetary Sciences, Purdue University, West Lafayette IN (melendl@purdue.edu), ²ARES, NASA JSC, Houston, TX, ³Jacobs, NASA JSC, Houston, TX, ⁴Stony Brook University, Stony Brook, NY.

Introduction: Space weathering, driven primarily by micrometeorite bombardment and solar wind ion irradiation, alters the morphology, microstructure, and chemistry of the surface regolith on airless bodies [1-3]. The accumulation of microstructural and chemical space weathering features, including melt deposits, amorphous rims, and nanophase iron-bearing particles (npFe), are associated with alterations of the spectral properties of the regolith. In particular, space weathering changes the spectral slope and reflectance of surface materials, and causes the attenuation of characteristic absorption bands in the visible to near-infrared wavelengths, as well as a shift towards longer wavelengths of the Christiansen feature (CF) in thermal infrared spectra [4,5]. Previous studies of space weathering characteristics have focused on siliceous bodies like the Moon and S-type asteroid Itokawa (6,7). However, observations of asteroid Ryugu by the JAXA Hayabusa2 spacecraft and subsequent analyses of returned samples revealed carbonaceous and hydrated materials. These samples provided our first opportunity to constrain the effects of space weathering processes on primitive, C-type asteroids [3,8-9]. Analyses of returned samples to understand the space weathering of carbonaceous materials are important for accurately interpreting remote sensing observations of carbonaceous asteroids. In addition, the analysis of Hayabusa2 samples from Ryugu paved the way for the analysis of samples from the asteroid Bennu, returned by the NASA OSIRIS-REx mission. As space weathering impacts the microstructure, chemistry, and spectral characteristics of asteroidal surfaces, here we report the results of a coordinated analytical study of the micro- and nano-scale signatures of space weathering in samples returned from Ryugu.

Samples: Five Ryugu particles returned by Hayabusa2 were allocated for this study: A0152, A0466, and A0512 from sample collection site A (representing surface material), and C0178 and C0428 collected from sample collection site C after the deployment of the small carry-on impactor. Our analysis focused on the bulk grain and associated subparticles (shed from the main sample mass during shipping due to the friable nature of these samples) for each particle.

Analytical Methods: We applied coordinated X-ray, electron microscopic, and nano-infrared techniques to these samples.

 μXCT : Each of the five particles were scanned via X-ray computed micro-tomography using the Nikon XTH 320 micro-XCT at NASA Johnson Space Center (JSC) with a resolution of 2.15 μ m/voxel. Higher-resolution sub-volume scans were also completed on the Zeiss Xradia 620 Versa at the University of Texas at Austin High Resolution X-ray CT Facility (UTCT) with a resolution of 0.79 μ m/voxel.

SEM-EDS: The main particle masses (~2 mm) and surface fragments (<500 μm) were transferred to C-tape on a scanning electron microscopy (SEM) mount and sputter coated with carbon. The prepared stubs were examined using the Hitachi TP 4000Plus SEM and the Thermo Scientific Helios G4 UX Dual Beam FIB-SEM at Purdue University for signatures of space weathering, including vesiculated impact melts. We extracted electron transparent cross sections of areas that exhibited evidence for space weathering from grain A0152, along with regions with no obvious signs of exposure for comparative purposes from grains A0152 and C0178.

S/TEM-EDS: We prepared four focused ion beam (FIB) sections from grain A0152 and two FIB sections from C0178. The FIB sections were analyzed using two scanning and transmission electron microscope (STEM) instruments, including (1) the JEOL 2500SE STEM at NASA Johnson Space Center (JSC) equipped with a 60 mm² ultra-thin window silicon drift detector (SDD) for energy-dispersive X-ray spectroscopy (EDS) analyses and bright field (BF), dark field (DF), and high-angle annular dark field (HAADF) STEM detectors and (2) the FEI Talos 200i STEM with a Super-X quad-SDD with EDS and on-axis Panther BF, DF, and HAADF detectors at Purdue University. Selected-area electron-diffraction (SAED) and high-resolution TEM (HRTEM) imaging was also used in both instruments for phase identification and analysis of sample crystallinity.

NanoIR: Two FIB sections that showed surface melt deposits from sample A0152 were mounted for analysis using the scattering-type scanning near-field optical microscopy (s-SNOM) combined with nanoscale Fourier transform infrared (nano-FTIR) spectroscopy instrument at the Center for Planetary Exploration at Stony Brook University. Nano-FTIR spectra were collected with ~20 nm spatial and 10 cm⁻¹ spectral resolution using a PtIr-coated neaspec cantilever tip (260 kHz tip frequency, ~90 nm tapping amplitude).

Results: Ryugu particles were first surveyed with XCT for surface evidence of micrometeorite bombardment in the form of microcraters. All of the particles were texturally diverse with a mix of fine- and coarsegrained matrix material, where brighter grayscale values correspond to denser materials. There are angular macroscale void spaces that can be identified inside the grain, reflective of the porous and fragile nature of the samples. The samples contain an abundance of high-density (bright) phases in hexagonal, planar shapes and framboidal morphologies, interpreted to be pyrrhotite and magnetite, respectively.

SEM and EDS analyses revealed grains were primarily composed of phyllosilicates with interspersed Fe-Ni sulfides, carbonates, and magnetite. Multiple subparticles (~10%) from Chamber A exhibited fine-scale vesiculated melt deposits measuring from 1-10 μm in diameter (Fig.1a), reminiscent of those found in simulated micrometeoroid bombardment experiments [10]. These localized melt deposits have also been observed in the recently returned samples from Bennu [11]. These melt splashes are attributed to micrometeoroid bombardment, indicating this particle was likely exposed on the surface of Ryugu.

The FIB sections extracted from these melt deposits reveal vesiculated melt layers (ranging from 100 nm to 1 μm in thickness) containing npFe and Fe-Ni-sulfide nanoparticles. The melt deposits are composed of predominantly silicate material with localized immiscible Fe-Ni-S melts. While the melts are chemically homogenous, there is noticeable depletion in S (70%) compared to the underlying materials, likely due to volatility. The vesicles (~50 to 80 nm) are heterogeneously distributed throughout the melt, with a majority of the vesicles occurring near the intersection of the melt and the underlying matrix, while others were spatially correlated with the walls of nano- and micro-scale inclusions seen in Fig. 1 b-e.

Nano-FTIR phase spectra acquired from the melt deposit and the matrix are shown in Fig. 2b. The spectra show evident water features at 1625 cm⁻¹ and carbonate features at 1440cm⁻¹, consistent with the composition of Ryugu particles. There are also phyllosilicate bands at ~1050 cm⁻¹ in the matrix, a feature absent in the melt layer spectra. Instead, there is a broader peak near 1150cm⁻¹, consistent with the glassy nature of the melt deposit. Future analysis will consist of investigating the remaining samples with electron microscopy and linking the nano-FTIR measurements with remote sensing observations.

Acknowledgments: This work was supported by NASA Award 80NSSC24M0171 to the co-authors. We thank JAXA for the allocation of Hayabusa2 samples.

References: [1] Pieters C.M. and Noble S.K. (2016) *JGR Planets*, 121:1865-1884. [2] Thompson et al. (2014) *Earth, Planets, and Space*, 66: 89. [3] Noguchi et al. (2023) *Nat. Astronomy*, 7:170–181. [4] Noble S.K. et al (2007) *Icarus* 192.2:629-641. [5] Kumari N. et al. (2024) *Icarus*,412: 115976. [6] Keller L.P. and McKay D. S. (1993) *Science*, 261:1305-1307. [7] Noguchi et al. (2011) *Science*, 333:1121-1125. [8] Hapke B. (2001) *JGR* 106:10039-10073. [9] Nakamura et al. (2011) *Science* 333:1113-1116. [10] Thompson M.S. et al. (2016) *Icarus*, 391:499-511. [11] Keller L. P. et al. (2024) *LPSC LV*, abs. 1399.

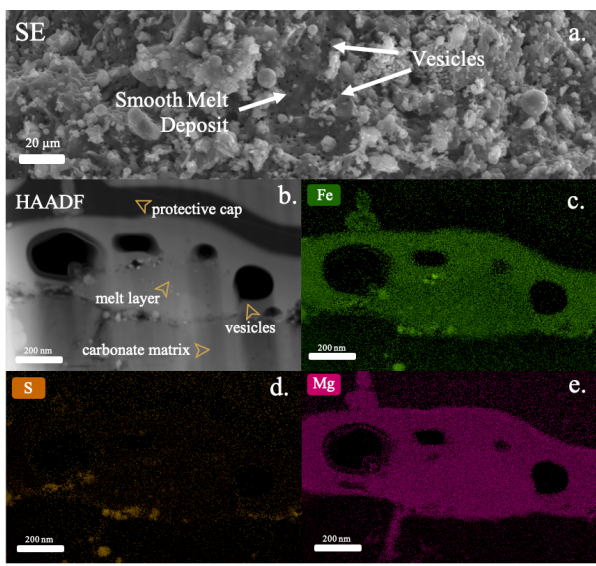
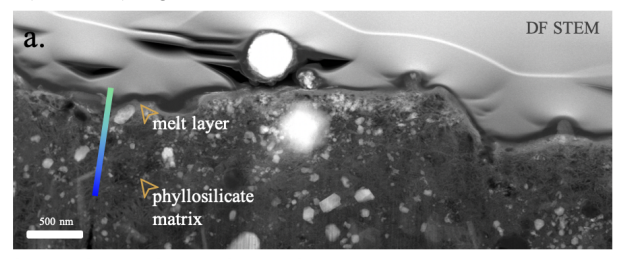
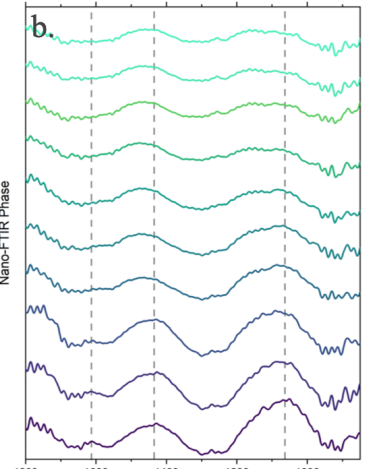


Figure 1. (a) Secondary electron (SE) SEM image of a melt deposit with abundant vesiculation across the surface of a subparticle of A0152. (b) HAADF image of the FIB section extracted from the space exposed particle A0152. The corresponding EDS for the following elements is shown in c) Fe, d) S, and e) Mg.





Wavenumber (cm⁻¹)

Figure 2. (a) DF STEM image of an extracted FIB section from a subparticle of A0152 with a phyllosilicate matrix with the line corresponding to the nano-FTIR phase spectra seen in (b). The water feature at 1625 cm⁻¹ increases with depth, suggesting dehydration at the surface.